Labial Mucosa Stem Cells: Isolation, Characterization, and Their Potential for Corneal Epithelial Reconstruction

Kirill E. Zhurenkov,[1,2] Elga I. Alexander-Sinkler,[1] Ilya O. Gavrilyik,[3] Natalia M. Yartseva,[1] Svetlana A. Aleksandrova,[1] Tatiana V. Mashel,[1] Julia I. Khorolskaya,[1] Miralda I. Blinova,[1] Alexei N. Kulikov,[3] Sergei V. Churashov,[3] Valery F. Chernysh,[3] and Natalia A. Mikhailova[1]

[1]Institute of Cytology Russian Academy of Science, St. Petersburg, Russia
[2]Department of Cytology and Histology, St. Petersburg State University, St. Petersburg, Russia
[3]S. M. Kirov Military Medical Academy, St. Petersburg, Russia

Correspondence: Kirill E. Zhurenkov, Institute of Cytology Russian Academy of Science, St. Petersburg 194064, Russia; kirill.zhurenkov@incras.ru.

KEZ and EIAS contributed equally to this work.

Received: January 12, 2022
Accepted: June 25, 2022
Published: July 18, 2022

Citation: Zhurenkov KE, Alexander-Sinkler EI, Gavrilyik IO, et al. Labial mucosa stem cells: Isolation, characterization, and their potential for corneal epithelial reconstruction. *Invest Ophthalmol Vis Sci.* 2022;63(8):16. https://doi.org/10.1167/iovs.63.8.16

Purpose. The purpose of this study was to characterize labial mucosa stem cells (LMSCs) and to investigate their potential for corneal epithelial reconstruction in a rabbit model of total limbal stem cell deficiency (LSCD).

Methods. Rabbit LMSCs (rLMSCs) and human (hLMSCs) LMSCs were derived from labial mucosa and characterized in terms of their proliferation activity by the evaluation of proliferation index (PI) and colony forming efficiency (CFE), cell senescence, and differentiation abilities. The expression of various limbus-specific, stem cell-specific, and epithelial markers was assessed via immunocytochemistry. Flow cytometry was used to evaluate mesenchymal and hematopoietic cell surface markers expression. Chromosomal stability of the derived cells was examined using the conventional GTG-banding technique. To assess the impact of LMSCs on corneal epithelial reconstruction, rLMSCs were seeded onto a decellularized human amniotic membrane (dHAM), thereafter their regeneration potential was examined in the rabbit model of total LSCD.

Results. Both rLMSCs and hLMSCs showed high proliferation and differentiation abilities, entered senescence at later passages, and expressed different stem cell-specific (ABCB5, ALDH3A1, ABCG2, and p63α), mesenchymal (vimentin), and epithelial (CK3/12, CK15) markers. Cell surface antigen expression was similar to other described mesenchymal stem cells. No clonal structural chromosome abnormalities (CSCAs) and the low percentage of non-clonal structural chromosome abnormalities (NSCAs) were observed. Transplantation of rLMSCs promoted corneal epithelial reconstruction and enhanced corneal transparency.

Conclusions. LMSCs have significant proliferation and differentiation abilities, display no detrimental chromosome aberrations, and demonstrate considerable potential for corneal repair.

Keywords: labial mucosa stem cells (LMSCs), cell characterization, limbal stem cell deficiency (LSCD), corneal regeneration, cornea

The cornea plays a crucial role in human vision. It participates in refraction and acts as a barrier protecting against a vast number of detrimental agents. The cornea has complex structure and is composed of six layers: an overlying epithelium, a Bowman's membrane, a corneal stroma comprising almost 90% of the whole tissue thickness, a Dua's layer, a Descemet's membrane, and an endothelium that is formed by a single layer of endothelial cells.[1,2] The maintenance of corneal integrity highly depends on its structure and functioning of the epithelium, which is constantly renewed by a population of limbal stem cells (LSCs). The LSCs inhabit specific limbal pockets within the corneal limbus and ensure corneal renewal in a physiological state and corneal restoration in a pathogenesis.[3,4] Disruption of the limbus may lead to LSC's death and cause limbal stem cell deficiency (LSCD) resulting in corneal opacity, vision loss, and even blindness. The main issue of LSCD treatment is that this disease is not always curable by commonly used methods.[5]

During the last few decades, there has been a significant increase in the development of various approaches aimed to restore damaged cornea from keratoplasty to tissue engineering and biofabrication.[6] Among tissue engineering approaches, the wide range of materials and stem cells has been used to design tissue-engineered graft with sufficient properties for corneal restoration.[6–9] However, the search for the appropriate cell source and materials is still ongoing.

LSCs are thought to be the gold standard for corneal restoration. However, either their harvesting or differentiation from induced pluripotent stem cells and other cell types have its own pros and cons.[10] In contrast to LSCs, one of the suitable cell sources could be oral mucosa due

Investigative Ophthalmology & Visual Science

to a simple procedure of tissue sourcing and similarities between corneal and oral mucosa epithelia. Particularly, buccal mucosa has been actively studied for the treatment of LSCD for several decades.[11–16]

Labial mucosa is another promising cell source that is also of ectodermal origin and is represented by nonkeratinized stratified squamous epithelium but, at the same time, has several advantages compared to buccal mucosa. Primarily, buccal mucosa is known to have parakeratinized and keratinized regions, such as linea alba.[17] Therefore, the use of buccal mucosa is potentially associated with contamination of the final culture with inappropriate cells and could possibly lead to the loss of LSCD treatment efficiency. Another benefit of labial mucosa is a simpler procedure of tissue sourcing in comparison to buccal mucosa.

In this study, we propose an efficient method of rabbit LMSCs (rLMSCs) and human LMSCs (hLMSCs) isolation, provide broad characteristics of both cell lineages, and emphasize the efficiency of rLMSCs transplantation for the treatment of LSCD. Both cell types were characterized in terms of their proliferative activity, chromosomal stability, senescence, expression of specific markers, and ability to differentiate into chondrogenic, adipogenic, and osteogenic lineages. Our results demonstrate that both rabbit and human LMSCs possess high proliferative activities and abilities to differentiate in a specific way. LMSCs have stable chromosomes with a low percentage of chromosome aberrations. We used rLMSCs seeded onto decellularized human amniotic membrane (dHAM) to restore damaged cornea in an animal model of LSCD. Importantly, it was shown that rLMSC-based tissue-engineered grafts promote corneal epithelial reconstruction with the re-epithelization in a cornea-like manner and the increase in corneal transparency.

Methods

Human Tissue Sourcing

Human labial mucosa tissue sourcing was performed under local administration of 2% lidocaine solution from healthy donors ($n = 8$; ages ranging from 20–30 years old; male:female donor ratio of 3:2). Amniotic membranes were obtained during planned Caesarean deliveries from healthy patients ($n = 5$). All procedures were performed following informed consent of use for research purposes.

Animals and Anesthesia

Three- to 4-month-old Soviet Chinchilla male and female rabbits (weighing 2.0–2.5 kg) were purchased from the Nursery of Laboratory Animals "Rappolovo" (St. Petersburg, Russia). The procedure of rabbit labial mucosa tissue sourcing was performed with the rabbits under local administration of 2% lidocaine solution. The construction of total LSCD and transplantation procedures were performed under local instillations of 0.5% alcaine solution (Alcon, Geneva, Switzerland) followed by retrobulbar administration of 2% lidocaine solution (1 mL). All animal experiments were approved by the Animal Welfare Assurance of the Institute of Cytology of the Russian Academy of Science (approval no. F18-00380) and the Ethics Committee of the S. M. Kirov Military Medical Academy (approval no. 212) and conducted in accordance with the Association for Research in Vision and Ophthalmology Statement for the Use of Animals in Ophthalmic and Vision Research.

Isolation and Culture of Labial Mucosa Stem Cells

Rabbit LMSCs were isolated from the upper labial mucosa, whereas human LMSCs were isolated from the lower labial mucosa according to the following protocol. Briefly, small samples (5 × 10 mm; 0.4 mm in a depth) of labial mucosa were mechanically dissected using no. 15 Bard Parker blade, washed 3 times with phosphate buffered saline (PBS) containing antibiotics (250 µg/mL gentamicin; 1000 U/mL Pen/Strep; Life Technologies, Carlsbad, CA, USA), and incubated in enzyme solution (5 mg/mL Dispase II; 12 mg/mL Collagenase type I; Sigma-Aldrich, St. Louis, MO, USA) in an ES-20 Orbital Shaker-Incubator (Biosan, Riga, Latvia) at 37°C for 40 minutes. Samples then were treated with 0.25% trypsin-EDTA (Life Technologies) at 37°C for 20 minutes, centrifuged for 7 minutes at 1200 × g, and the final cell suspension was plated in a culture dish. The labial mucosa-derived cells were cultured in DMEM/F-12 medium (Life Technologies) supplemented with 10% of fetal bovine serum (FBS; Cytiva, Marlborough, MA, USA), 1000 U/mL Pen/Strep (Life Technologies), and 0.5 ng/mL amphotericin B (Thermo Scientific, Waltham, MA, USA) in an incubator at 37°C, 5% CO_2, and 95% humidity. One to 2 weeks after isolation, both rLMSCs and hLMSCs were tested for mycoplasma contamination. After reaching 70% to 80% confluency, cells were passaged using 0.25% trypsin-EDTA for 3 minutes at 37°C and cultured up to passage 6 for further in vitro or in vivo studies.

Cell Proliferation Assay

The proliferation index (PI) was estimated to determine proliferative rates of both rLMSCs and hLMSCs, as described previously.[18] Briefly, 5×10^4 cells were seeded on 3 cm Ø Petri dishes and cultured in the supplemented DMEM/F-12 medium for 6 days. Cell counting was performed every 24 hours using a Countess II FL Automated Cell Counter (Thermo Scientific), hereupon, the average population doubling time of each of the cell lineages was measured and growth curves were plotted.

Colony Forming Assay

A colony forming assay was performed as previously reported.[19] Cells were seeded with small densities (80–100 cells per 5 cm Ø Petri dishes) and cultured for 2 weeks. Grown colonies were then fixed in 70% ethanol and stained with Crystal Violet (Lenreaktiv, St. Petersburg, Russia). Colonies with at least 50 cells were counted. The colony forming efficiency (CFE) was calculated as the ratio of the number of colonies grown to the number of cells seeded.

Senescence Associated-β-Galactosidase Staining

Cell senescence assay was performed using Senescence β-Galactosidase Activity Assay Kit (Cell Signaling, Danvers, MA, USA) according to the manufacturer's protocol. Senescence associated-β-galactosidase (SA-β-galactosidase) activity was estimated every 2 passages from 6 to 20. A number of SA-β-galactosidase positive cells were assessed using the ImageJ version 2.1 software.

Investigative Ophthalmology & Visual Science

Multilineage Differentiation

The abilities of both rLMSCs and hLMSCs to differentiate into chondrogenic, adipogenic, and osteogenic lineages were determined using StemPro Chondrogenesis, Adipogenesis, and Osteogenesis Differentiation Kits (Thermo Scientific), respectively, according to the manufacturer's protocols. Differentiation media were changed every 3 to 4 days, cells cultured in the complete DMEM/F12 medium were used as a control. For chondrogenic differentiation, 1×10^6 cells were pelleted in centrifuge tubes and incubated in a micromass culture for 3 weeks in the differentiation medium. To detect chondrogenic differentiation, cytologic smears were prepared from micromass formed, fixed in 4% paraformaldehyde (PFA) in PBS at room temperature for 20 minutes, and separately stained with 1% Toluidine Blue, 1% Alcian Blue, and 0.1% Safranin O solutions (Lenreaktiv) for 30 minutes at room temperature. To induce adipogenic and osteogenic differentiation 2×10^4 cells were plated in 24-well plates and cultured in the differentiation media for 4 weeks. Cells then were fixed in 4% PFA for 20 minutes and stained with either Nile Red (Invitrogen, Waltham, MA, USA) at 37°C for 10 minutes or Alizarin Red S Staining Kit (ScienCell, Carlsbad, CA, USA) at room temperature for 30 minutes to detect adipogenic and osteogenic differentiation, respectively. Nuclei were stained with DAPI (Sigma-Aldrich) for 2 to 3 minutes at room temperature. The mean area of lipid droplets and alizarin-positive staining was assessed using the ImageJ version 2.1 software.

Immunostaining

Both rLMSCs and hLMSCs (1×10^4) were seeded on cover glasses and cultured in 24-well plates in the supplemented DMEM/F-12 medium for 2 to 3 days. Cells then were washed 3 times with PBS, fixed with 4% PFA for 20 minutes, washed again with PBS, permeabilized with 0.1% Triton X-100 for 15 minutes, blocked in PBS supplemented with 1% bovine serum albumin (BSA; Thermo Scientific) at 37°C for 1 hour, and incubated overnight at 4°C with primary antibodies (Supplementary Table S1) diluted in PBS-Tween20 (PBST; Thermo Scientific) according to the manufacturer's recommendations. Thereafter, cells were washed 3 times with PBST, incubated for 2 hours at room temperature with the corresponding secondary antibodies in PBST, washed again with PBST, stained with DAPI for 2 to 3 minutes, washed 3 times with PBST, and mounted onto glass slides. Images were collected using an OLYMPUS FV3000 confocal microscope (Olympus, Tokyo, Japan). Data were processed and analyzed using the ImageJ version 2.1 software.

Flow Cytometry

Characterization for mesenchymal and hematopoietic cluster of differentiation (CD) antigens was performed by flow cytometry using specific antibodies conjugated either with phycoerythrin (PE) or fluorescein isothiocyanate (FITC) in the dilutions according to the manufacturer's recommendations (Supplementary Table S2). Before examination, both rLMSCs and hLMSCs (1×10^6) were resuspended in 1 mL of PBS and separately stained with appropriate primary conjugated antibodies in the dark at room temperature for 60 minutes. The stained cells were diluted with PBS (1:10) and examined using a CytoFLEX Flow Cytometer (Beckman Coulter, Brea, CA, USA). Isotypes of PE (Iso PE) and FITC (Iso FITC) were used as negative controls.

Cytogenetic Analysis

Karyotypes of both rLMSCs and hLMSCs were analyzed to confirm chromosomal stability of the derived cells. Cells (2×10^5) were seeded on 10 cm Ø Petri dishes, cultured in the supplemented DMEM/F-12 medium for 2 to 3 days, and treated with colchicine (0.06 µg/mL; Sigma-Aldrich) for 1.5 and 2.5 hours, respectively. Cells then were washed 3 times with PBS, trypsinized (enzyme activity was blocked with FBS), resuspended in PBS, and centrifuged at 1000 × g for 5 minutes. Samples of metaphase chromosomes were collected as described previously.[20] Briefly, the supernatant was gently removed, rLMSCs and hLMSCs were treated with hypotonic solution (0.075 M KCl and 1% Na-citrate 1:1, respectively; Sigma-Aldrich) at 37°C for 20 and 25 minutes, respectively, with the following 2-step cycle repeated 3 times: centrifugation at 1000 × g for 5 minutes, fixation in the mixture of absolute methanol and glacial acetic acid (3:1; Sigma-Aldrich). Thereafter, cell suspensions were spread onto glass slides over water bath. Metaphase patterns were subjected to the conventional trypsin GTG-banding technique[20,21] and analyzed under a ZEISS Axio Scope.A1 microscope (Carl Zeiss, Oberkochen, Germany) using × 100 immersion objective (NA = 1.3). Cytogenetic characterization was performed according to the international chromosome G-band rabbit and human nomenclatures.[22,23] Karyotypes were processed using VideoTest-Karyo version 3.1 (ArgusSoft, St. Petersburg, Russia). For both cell lineages, 500 and 100 metaphase patterns were analyzed for polyploidy and chromosome aberrations, respectively.

Human Amniotic Membrane Preparation

The dHAMs were prepared from human placentas obtained during planned Caesarean deliveries and processed at S. M. Kirov Military Medical Academy (St. Petersburg, Russia), as previously reported.[24,25] Briefly, amniotic membranes were mechanically separated from the chorion, washed in Ringer's solution containing ceftriaxone (10 mg/mL; Sintez, Moscow, Russia), fixed onto 3 cm Ø Petri dishes without bottoms under sterile conditions, and cryopreserved at –80°C in a mixture of DMEM/F12 medium and dimethyl sulfoxide (1:1) (DMSO; BioloT, St. Petersburg, Russia). Before further use, dHAMs were thawed at 37°C, washed 3 times with PBS, and decellularized at 37°C for 45 minutes using 0.25% Trypsin-EDTA.

Rabbit LSCD Model

A total number of 30 rabbits were subjected to the ocular surgery (right eyes). To create the total LSCD model conjunctival and corneal tissues were excised to 2 mm outside limbus and then the whole limbus (having 4 mm in a width and 0.2 mm in a depth) was removed using a beveled corneal microblade. The remaining corneal epithelium was scraped off using the same microblade. Tobradex (Novartis, Basel, Switzerland) and 5% corneregel (Bausch Health, Quebec, Canada) solutions were applied to the eyes immediately after surgery and then were administered 4 times a day for 2 weeks.

Graft Transplantation Protocol

Rabbits with the total LSCD were divided into 3 groups: one with 10 animals subjected to the transplantation of dHAM (control group); a second group with 10 animals subjected to the transplantation of rLMSCs seeded onto dHAM with the membrane facing up and the cells facing down (rLMSCs-down); and a third group with 10 animals subjected to the transplantation of rLMSCs seeded onto dHAM with the membrane facing down and the cells facing up (rLMSCs-up; see Supplementary Fig. S1 for the experimental design). Before transplantation, 360 degrees conjunctival peritomy was performed to the right eyes of all animals and the fibrovascular pannus was removed. Then grafts were placed on the prepared corneas and secured with interrupted 8–0 nylon sutures through their edges to the episclera.

Graft Transplantation Assessment

The graft's opacity score, neovascularization score, and epithelization score were assessed using a slit-lamp biomicroscope at 7, 15, 30, 60, and 90 days. The degree of corneal opacity was scored as follows: 1 to 2, total transparency; 3, moderate transparency; 4 to 5, weak transparency; and 6 to 10, opacity.[26] The degree of corneal neovascularization was scored as follows: 0 = lack of neovascularization; 1 = sparse peripheral neovascularization at the side of the limbus (up to 2 mm); 2 = strong peripheral neovascularization at the side of the limbus (up to 4 mm); 3 = total limbal neovascularization and sparse corneal neovascularization; and 4 = total corneal neovascularization.[27] To estimate the degree of corneal epithelization, rabbit eyes were stained with 1% fluorescein sodium solution and photographed under blue light. Images then were processed using 385-meshes radial grid (1 mesh approximately 0.26%) in the Adobe Photoshop Lightroom 5 (Adobe, San Jose, CA, USA) and the fluorescein-free meshes were calculated to assess the corneal epithelization.[28]

Histological Analysis

The efficiency of corneal regeneration was assessed in all three groups via histological analysis of the corneal integrity, the number of new blood vessels formed per mm^2 across limbal region and corneal stroma, and the presence of inflammatory cells. For these purposes, 9 whole rabbit eyes (from 3 animals of each group at 3 months after transplantation) were fixed in 4% PFA for 3 days. After that, corneal rings with adjacent sclera were mechanically dissected, embedded in paraffin, and cut into 4-µm-thick tissue sections. Thereafter, tissue sections were subjected to either the hematoxylin and eosin (H&E) or Alcian Blue (Lenreaktiv) staining and examined using bright-field microscopy.

Statistical Analysis

In all experiments, at least three independent measurements were performed. Error bars are represented as the standard deviation (SD) of the mean, and analyzed a priori for homogeneity of variance. Replicates from each independent experiment were confirmed to follow a Gaussian distribution. Differences between groups were determined using Welch's *t*-test (CFE, SA-β-galactosidase positive cells, and bone-like matrix deposition area) and 1-way or 2-way analysis of variance (ANOVA) followed by Tukey's multiple comparison post hoc test (PI, LDs area, opacity score, neovascularization score, epithelization score, and blood vessels number). Significance between groups was established for $P < 0.05$, $P < 0.001$, $P < 0.0002$, and $P < 0.0001$ with a 95% confidence interval. All statistical calculations and graphs plotting were performed using Prism version 9.0 (GraphPad Software, San Diego, CA, USA).

Results

In Vitro Cultures of rLMSCs and hLMSCs

The rLMSCs and hLMSCs primary cultures were represented by the heterogeneous populations of hexagonal epithelial-like cells and elongated mesenchymal-like cells (Fig. 1A). During long-term culturing mesenchymal-like cells became predominant resulting in the homogeneous culture which maintained after passaging and cryopreservation (see Fig. 1A).

The derived cell lineages possessed significant proliferative activities at passage (P) 6 with the long phases of fast growth (96 hours) and the mean population doubling time of 36.03 ± 1.07 hours and 36.22 ± 1 hours for rLMSCs and hLMSCs, respectively (Fig. 1B). Although both cell lineages showed high proliferative rates, hLMSCs (42% ± 4.9) had lower CFE in comparison to rLMSCs (62.5% ± 3.8; Fig. 1C).

rLMSCs and hLMSCs Entry Senescence at Later Passages

Cell senescence was assessed via SA-β-galactosidase activity (Fig. 2, Supplementary Fig. S2). At the early passages, both rLMSCs and hLMSCs showed minor SA-β-galactosidase activity (see Fig. 2A). In case of rLMSCs, it remained almost at the same level during long-term culturing both at P20 (see Fig. 2A) and later passages (data not shown) having 5.62% ± 0.63 of SA-β-galactosidase positive cells (Fig. 2B) which maintained their proliferative activities. Compared to the rabbit cells, hLMSCs entered senescence at P20 having 25.03% ± 4.02 of SA-β-galactosidase positive cells (Figs. 2A, 2B).

rLMSCs and hLMSCs Differentiate Into Adipogenic, Osteogenic, and Chondrogenic Ways

To confirm the multipotency of the derived cell lineages, rLMSCs and hLMSCs were differentiated in vitro using chondrogenic, adipogenic, and osteogenic differentiation media (Fig. 3). Cells cultured alongside under standard conditions in the complete DMEM/F-12 medium were used as a control.

Chondrogenic differentiation was performed in the micromass culture. At the end of the differentiation period, both rLMSCs and hLMSCs formed a dense micromass (3–4 mm in a diameter) with the higher amount of extracellular matrix which was positively stained for proteoglycans and different glycosaminoglycans (see Fig. 3A) widely represented in cartilage tissue.

When cultured in the adipogenic differentiation medium, both rLMSCs and hLMSCs displayed significant morphological changes. Cells acquired larger shape, whereas massive lipid droplets (LDs; 2.14 ± 3.16 μm^2 and 3.32 ± 3.86 μm^2 for rLMSCs and hLMSCs, respectively) were observed in their cytoplasm by the end of the differentiation period (Figs. 3B, 3C).

Investigative Ophthalmology & Visual Science

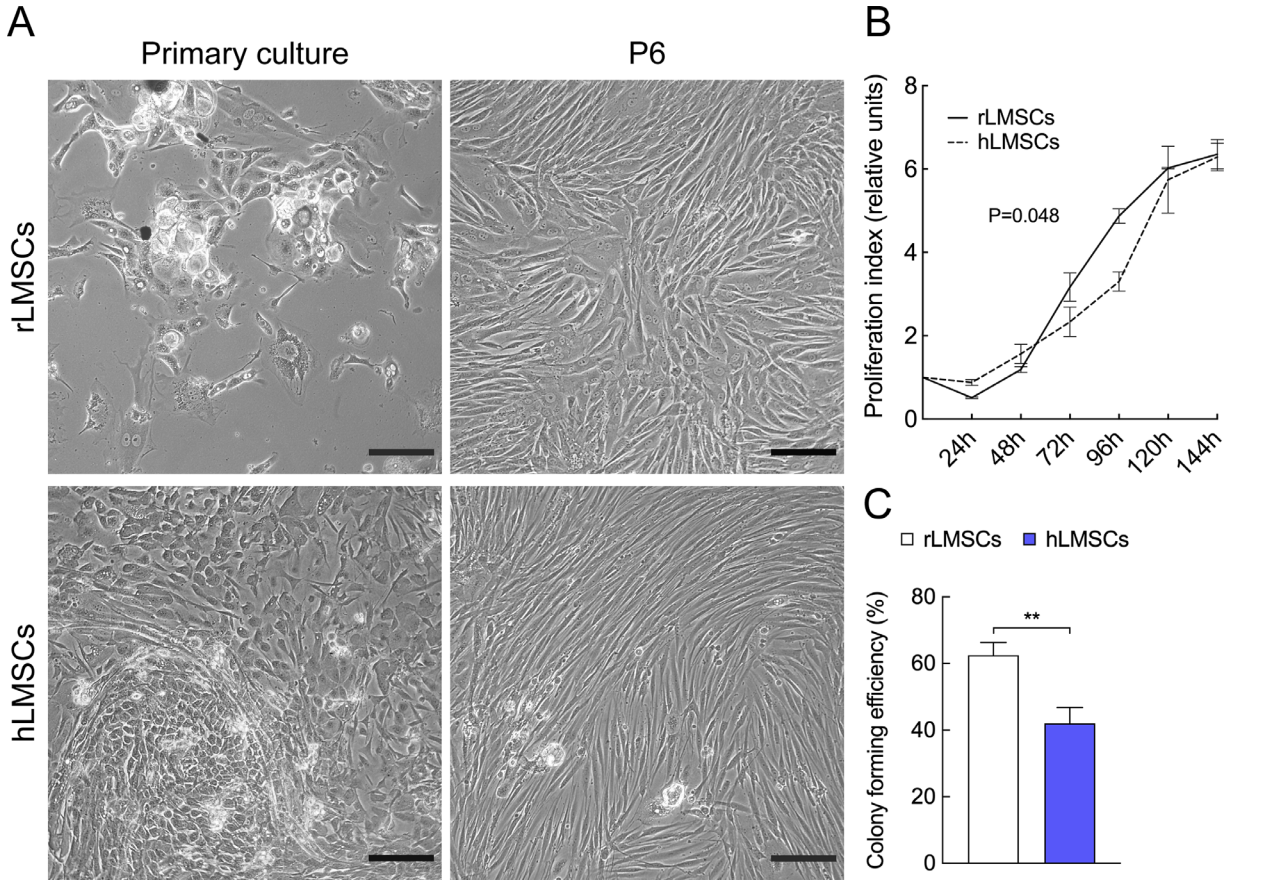

Figure 1. Growth potential and in vitro cultures of rLMSCs and hLMSCs. (**A**) Primary cultures of the derived cell lineages were represented by both epithelial-like cells and mesenchymal-like cells which became predominant during long-term culture. (**B**) Growth curves of rLMSCs and hLMSCs at P6 ($n = 3$; $P = 0.048$). (**C**) Colony forming efficiencies of rLMSCs and hLMSCs at P6 ($n = 3$; $^{**}P < 0.001$). Data are presented as the means ± SD. Scale bars: 300 µm.

When cultured in the osteogenic differentiation medium, LMSCs elongated and the formation of the high amount of bone-like extracellular matrix was observed via Alizarin Red staining (Figs. 3D, 3E).

rLMSCs and hLMSCs Express Stem Cell-Specific and Epithelial Markers

The derived cell lineages of rLMSCs and hLMSCs were characterized via immunocytochemistry for the expression of epithelial, stem cell-specific, and mesenchymal markers (Fig. 4, Supplementary Table S3). Particularly, p63α, PAX6, ABCG2, and CK3/12 expression was examined to detect markers which are commonly used in a description of LSCs and other corneal cells.

Both cultures of rLMSCs and hLMSCs showed strong positivity for CK15 and moderate positivity for CK3/12 with filaments formed in rLMSCs cytoplasm (see Fig. 4A). Meanwhile, the expression of CK5, CK14, and CK19 was only observed across multilayered epithelial colonies within primary culture of hLMSCs (Supplementary Fig. S3). Simultaneously, cells expressed vimentin that is commonly used as a mesenchymal marker (see Fig. 4B).

Strong expression of stem cell-specific markers, which are commonly used in a description of the vast number of progenitor and stem cells, such as ABCB5, ALDH3A1, nestin, NGFR (p75), and integrin β1 was found in both cell cultures (see Fig. 4C).

The expression of nuclear transcriptional factor p63α and ABC transporter ABCG2 was observed in both cell lineages of rLMSCs and hLMSCs although the signals were not significantly strong (see Supplementary Fig. S3). PAX6 expression was found only in rLMSCs nuclei, and no expression was found in hLMSCs (see Supplementary Fig. S3).

rLMSCs and hLMSCs Display Mesenchymal Cell Surface Markers Expression

The rLMSCs and hLMSCs were examined for the expression of the commonly used mesenchymal (e.g. CD44, CD73, CD90, and CD105), hematopoietic (e.g. CD34 and CD45), and other specific markers (Fig. 5, Supplementary Table S4). Due to the lack of antibodies that specifically interact with rabbit antigens, antibodies against human antigens were used to detect any cross-reactivity.

Both cultures of rLMSCs and hLMSCs had the significant number of CD44 (68.47% ± 2.23 and 99.30% ± 0.41 – respectively) and CD90 (89.69% ± 0.77 and 98.36% ± 1.76) positive cells. CD105 was expressed much higher in the population of hLMSCs (96.61% ± 5.16 against 27.18% ± 14.89) whereas CD73 expression was observed only in the population of hLMSCs (90.08% ± 16.83 against 5.98% ± 7.05; see

Investigative Ophthalmology & Visual Science

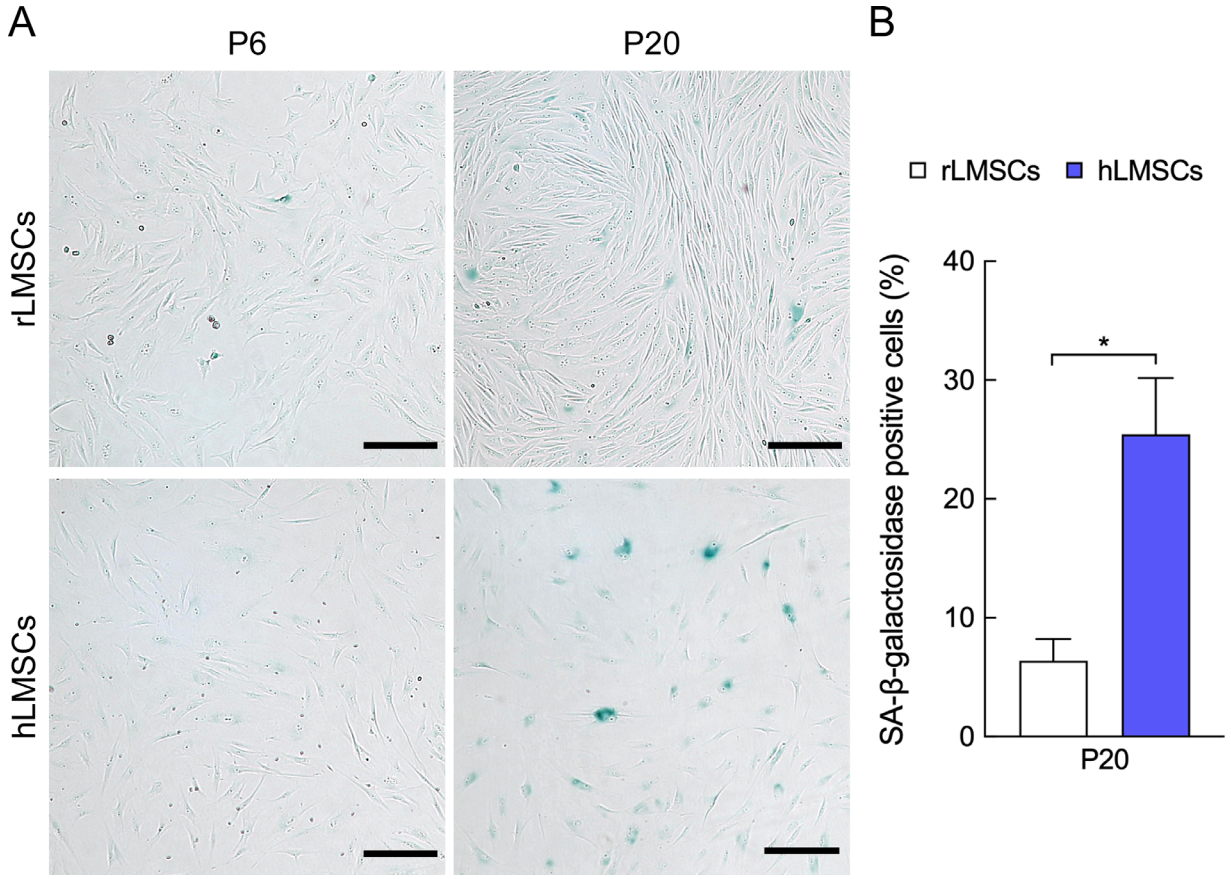

Figure 2. Senescence features of rLMSCs and hLMSCs during long-term culture. (**A**) Cells displayed negligible SA-β-galactosidase activity at P6 which increased markedly in the culture of hLMSCs to P20. (**B**) Percentage of rLMSCs and hLMSCs positively stained for SA-β-galactosidase at P20 ($n = 3$; $^*P < 0.05$). Scale bars: 200 µm.

Fig. 5A). The expression of hematopoietic markers such as CD34 (0.87% ± 0.95 and 0.45% ± 0.11), CD45 (5.47% ± 6.54 and 0.95% ± 0.45), and CD117 (2.79% ± 1.16 and 0.99% ± 1.46) was not found in both cell lineages. In addition, the endothelial marker CD146 (7.67% ± 1.86 and 0.63% ± 0.59) was not expressed widely (see Supplementary Table S4).

It should be noted that both rLMSCs and hLMSCs expressed endothelial and epithelial marker CD13 (66.14% ± 0.76 and 99.39% ± 0.5). In addition, LMSCs were positive for fibroblasts and mesenchymal marker CD140b (91.07% ± 0.17 and 31.76% ± 3.53) which expression corresponds to cell proliferation, differentiation, and survival (see Fig. 5C).[29]

rLMSCs and hLMSCs Maintain Chromosomal Stability

In the field of regenerative medicine, chromosomal stability of transplanted stem cells are thought to be a crucial point for successful tissue regeneration without any risks for patient's health, including the possibility of cells' oncogenic transformation. Therefore, LMSCs were examined for possible chromosomal instability via karyotype analysis at P6.

Karyotypes of both cell lineages were found to be normal (2n: rLMSCs – 44,XX; rLMSCs – 46,XY), meanwhile the number of polyploid cells was accounted for 6.4% and 2.9% for rLMSCs and hLMSCs, respectively (Fig. 6). Importantly, no cells with the numerical chromosome alterations as well as with CSCAs were observed.

Non-clonal structural chromosome abnormalities (NSCAs) were accounted for 6% in the population of rLMSCs and were represented with chromatid breaks of chromosomes 5, 7, and 8 (at loci 5p13, 7p22, and 8q22), chromosomal break of chromosome 15 (at locus 15q23), and deletions of chromosomes 12 and 20 (del(12)(q21:); del(20)(q14:)). In addition, there was found one cell with 2 NSCAs: chromatid breaks of chromosomes 5 and 15 (at 5p13 and 15q23, respectively; see Fig. 6A). In comparison to rabbit cells, hLMSCs had lower portion of cells with NSCAs accounted for 2%: chromatid break of chromosome 4 – chtb(4)(q?23) and deletion of chromosome 6 – del(6)(p?15:) (see Fig. 6B).

rLMSCs Promote Corneal Epithelial Reconstruction in the Rabbit Model of LSCD

The transplantation of rLMSCs seeded onto dHAM was performed to assess their impact on corneal epithelial reconstruction after severe damage in the rabbit model of total LSCD (Fig. 7).

A week after transplantation, corneas in all three groups lost transparency (see Fig. 7A) and the opacity score (control, 5.9 ± 0.74; rLMSCs-down, 3.8 ± 0.63; rLMSCs-up, 6.5 ± 1.08, $P = 0.0794$, compared to the control) increased significantly

Investigative Ophthalmology & Visual Science

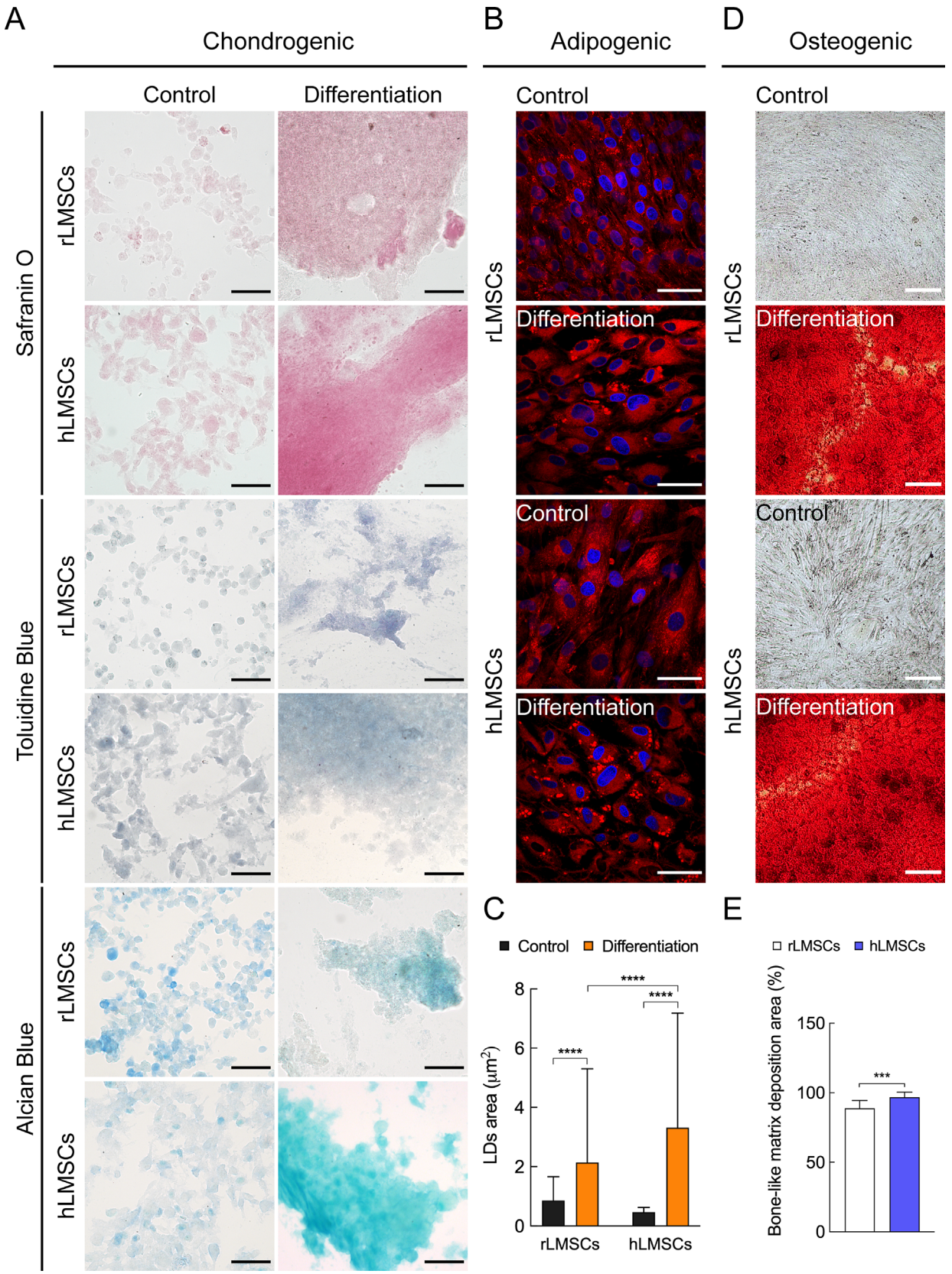

Figure 3. Differentiation potential of rLMSCs and hLMSCs. (**A**) Safranin O, Toluidine Blue, and Alcian Blue staining for chondrogenic differentiation at P6 after 3 weeks of culturing. (**B**) Nile Red staining for adipogenic differentiation at P6 after 4 weeks of culturing (nuclei were stained with DAPI). (**C**) Significantly larger LDs formed in the differentiated cells ($n > 100$; $^{****}P < 0.0001$). (**D**) Alizarin Red staining for bone-like extracellular matrix deposition at P6 after 4 weeks of culturing. (**E**) LMSCs produced the high amount of bone-like extracellular matrix by the end of the osteogenic differentiation ($n = 10$; $^{***}P < 0.0002$). Scale bars: 50 µm (**A, B**), 200 µm (**D**).

Investigative Ophthalmology & Visual Science

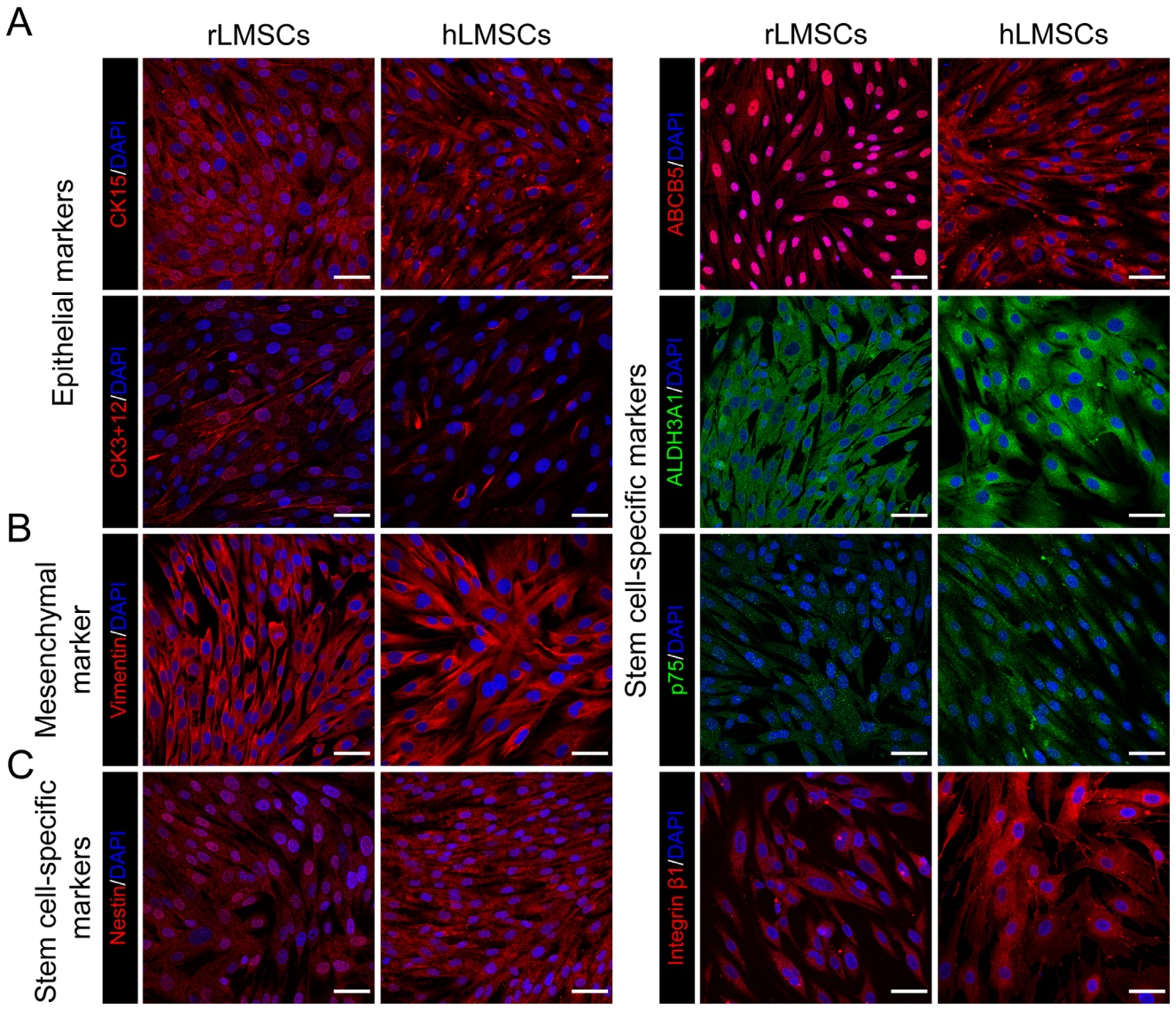

Figure 4. The rLMSCs and hLMSCs display stem cell-specific, mesenchymal, and epithelial markers expression. Both cultures of rLMSCs and hLMSCs showed the positivity for epithelial (**A**), mesenchymal (**B**), and stem cell-specific markers (**C**). Scale bars: 50 µm.

(see Fig. 7B). In 15 days, the opacity score in the rLMSCs-up grafts group (control, 7.8 ± 0.79; rLMSCs-down, 7.1 ± 0.74; rLMSCs-up, 4.3 ± 0.67, $P < 0.0001$, compared to the control) reduced and continued to decrease in the following weeks, whereas in the other two groups, a sufficient improvement of corneal clarity was not observed.

The neovascularization score witnessed similar tendency. It increased in all 3 groups almost throughout the entire period with the rLMSCs-up grafts group having the maximum in 30 days (control, 3.5 ± 0.85; rLMSCs-down, 3.5 ± 0.71; rLMSCs-up, 2.5 ± 0.53, $P < 0.0002$, compared to the control) followed by a gradual decline (see Fig. 7C).

Corneal epithelization was achieved in all 3 groups during 5 weeks after transplantation (see Fig. 7D). It should be noted that in the rLMSCs-up grafts group corneal epithelization was achieved earlier in comparison to other groups (day 7: control, 52.39% ± 1.97; rLMSCs-down, 41.97% ± 2.34; rLMSCs-up, 98.46% ± 0.58, $P < 0.0001$, compared to the control).

Importantly, both the opacity (day 90: control, 4.8 ± 0.42; rLMSCs-down, 5.2 ± 0.42; rLMSCs-up, 1.6 ± 0.52, $P < 0.0001$, compared to the control) and neovascularization (day 90: control, 3.8 ± 0.42; rLMSCs-down, 3.9 ± 0.32; rLMSCs-up, 2.3 ± 0.48, $P < 0.0001$, compared to the control) scores were significantly lower in the rLMSCs-up grafts group in 90 days after transplantation (see Figs. 7B, 7C).

The epithelization in a cornea-like manner with stratified squamous epithelium formed was observed in the rLMSCs-up grafts group in 90 days after transplantation in comparison to the control and the rLMSCs-down grafts groups where the expansion of conjunctival goblet cells-enriched epithelium was found (Fig. 8, Supplementary Fig. S4). It should be noted that the fibrosis of upper layers as well as the presence of inflammatory cells (mainly eosinophils) were found across corneal stroma in all 3 groups in 90 days after

Investigative Ophthalmology & Visual Science

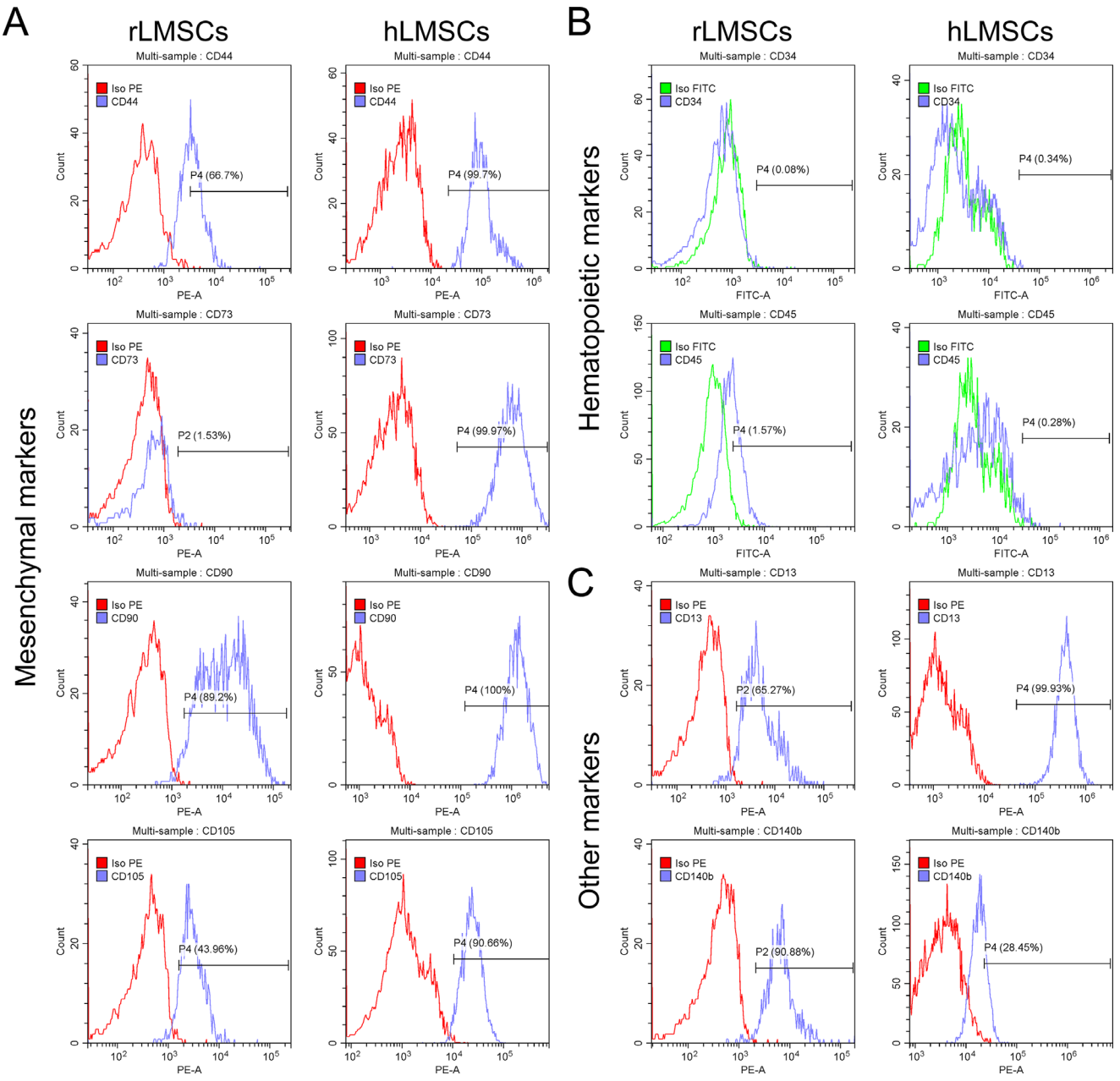

Figure 5. The rLMSCs and hLMSCs express specific mesenchymal cell surface markers. Both cultures of rLMSCs and hLMSCs expressed mesenchymal cell surface markers (**A**) whereas the expression of hematopoietic markers was negligible (**B**). Additionally, the expression of epithelial marker CD13 and mesenchymal marker CD140b was observed in both cell lineages (**C**). Iso PE (red) and Iso FITC (green) were used as negative controls.

transplantation (see Fig. 8A). Neovascularization of corneal stroma appeared to be as the increase in the number of newly formed blood vessels per mm^2 in all three experimental groups of animals (see Fig. 8B). However, there were no statistically significant differences in the rLMSCs-up grafts group (native cornea, 0; LSCD, 6.3 ± 0.6; control, 3.5 ± 0.5; rLMSCs-down, 4 ± 1; rLMSCs-up, 3 ± 1, $P = 0.0017$, compared to native cornea) in comparison to native cornea, which could be associated with the chosen sample size.

Corneal limbus is usually supplied by the vast number of blood vessels, which is crucial for its functions. We observed a reduction in the number of blood vessels per mm^2 across the limbal region in the control, rLMSCs-down, and rLMSCs-up grafts groups (see Fig. 8B). Again, there were no statistically significant differences in the rLMSCs-up grafts group (native cornea, 11 ± 2; LSCD, 5 ± 0.6; control, 4.5 ± 0.5; rLMSCs-down, 4.5 ± 1.5; rLMSCs-up, 5.5 ± 0.5, $P = 0.014$, compared to native cornea) in comparison to native cornea, which could be associated with the chosen sample size. Nevertheless, the apparent reconstruction of the limbus integrity, including the restoration of the limbal stem and adjacent goblet progenitor cells niches after surgery, was not achieved in all three groups with an exemption for the third rabbit from the rLMSCs-up grafts group, which showed the increase in the number of goblet cells across limbal region (see Supplementary Fig. S4).

Investigative Ophthalmology & Visual Science

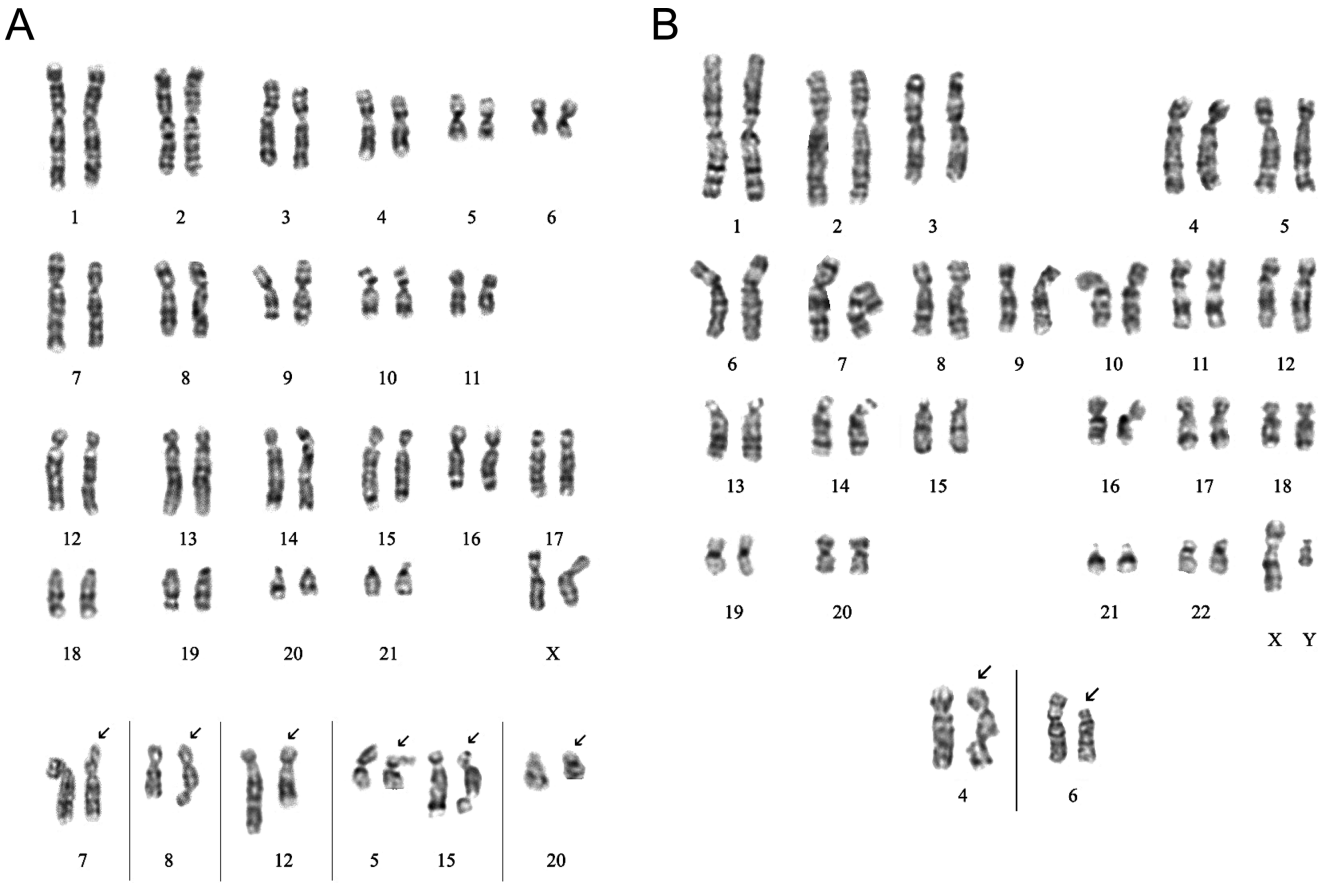

Figure 6. The rLMSCs and hLMSCs have stable genomes. (**A**) Normal G-banded karyotype of rLMSCs. NSCAs (on inset represented NSCAs from different cells, indicated with arrows) were accounted for 6% of the examined metaphase patterns: chromatid breaks of chromosomes 5, 7, 8, and 15 (at 5p13, 7p22, 8q22, and 15q23), deletions of chromosomes 12 – del(12)(q21:) and 20 – del(20)(q14:). (**B**) Normal G-banded karyotype of hLMSCs. NSCAs (on inset represented NSCAs from different cells, indicated with arrows) were accounted for 2% of the examined metaphase patterns: chromatid break of chromosome 4 – chtb(4)(q?23), deletion of chromosome 6 – del(6)(p?15:).

Discussion

LSCD is thought to be one of the most challenging corneal diseases to diagnose and relates to the disruption of LSCs niche causing corneal opacity and vision loss.[30] Therefore, the vast number of stem cells and materials has been investigated for LSCD treatment purposes during the last several decades.[6] The first case of oral mucosa tissue sheets use for the treatment of eye burns was shown by Ballen in the early 1970s.[11] In the more recent studies, Nakamura et al. reported the first successful application of oral mucosa stem cells grown on the amniotic membrane for the treatment of ocular surface injury in rabbits.[12] Finally, the use of either oral mucosa tissue sheets or oral mucosa stem cells for the treatment of LSCD were confirmed by different authors in the following years.[15,16,31] However, to our best knowledge, there was not enough data on the characteristics of LMSCs in regard to the specific markers' expression, differentiation, and especially chromosomal stability in vitro that should be of paramount importance for stem cells proposed for using in regenerative medicine.[32]

Herein, we described cultures of both rabbit and human LMSCs. Particularly, the description of not only hLMSCs but also rLMSCs seems to us crucial as model cells used for the treatment of LSCD in rabbits.

We demonstrated that both rLMSCs and hLMSCs had high proliferation rates, ability to differentiate into chondrogenic, adipogenic, and osteogenic ways, and entered senescence at later passages that is quite common among mesenchymal stem cells derived from different tissues.[18,33] Interestingly, rLMSCs displayed fewer SA-β-galactosidase activity even after long-term culturing (P30). This could be associated with the fact that animal cells are known to escape senescence at later passages, whereas in human cells, it is strictly controlled.[34] Compared to rabbit cells, hLMSCs became aged after P8 having around 10% of senescent cells at P10 (see Supplementary Fig. S2). Therefore, it could be recommended to use hLMSCs up to P12 to ensure the greater efficiency of corneal epithelial reconstruction.

We found that both cultures of rLMSCs and hLMSCs had the expression of the wide range of different markers described as specific for various stem and progenitor cells.[35,36] Particularly, both rLMSCs and hLMSCs expressed nuclear transcriptional factor p63α and ABC transporter ABCG2, whereas the expression of melanoma-associated chondroitin sulfate proteoglycan N/MSCP, previously shown for buccal mucosa cells,[37] was not observed which could be associated with the differences among subpopulations of oral mucosa cells. Interestingly, the expression of PAX6, usually associated with eye development during organogenesis,[38] was found only in rLMSCs. It should be noted

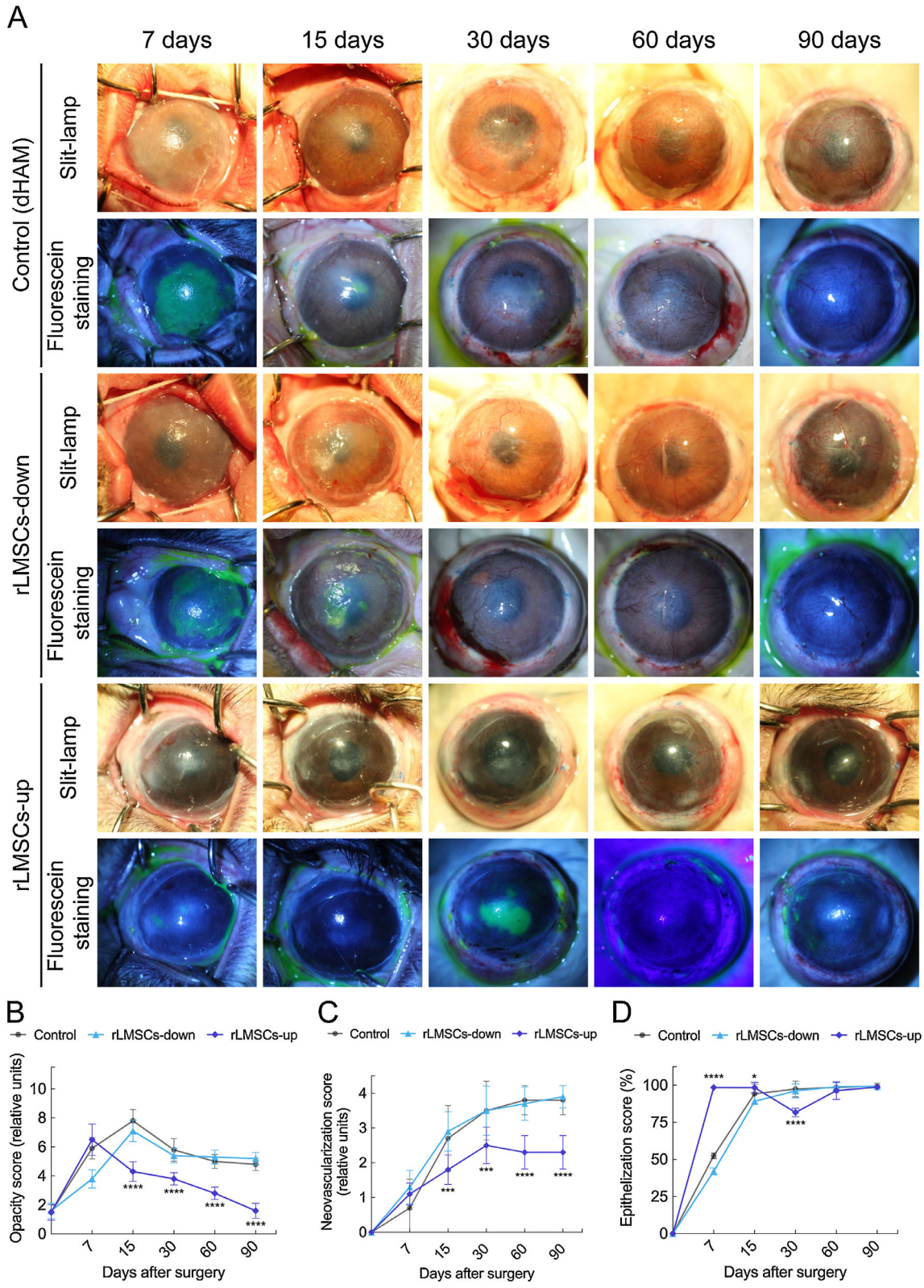

Figure 7. The rLMSCs-up transplantation promotes corneal epithelization and enhances corneal clarity. Representative slit-lamp and fluorescein sodium staining biomicroscope images of rabbit corneas at 7, 15, 30, 60, and 90 days after surgery (**A**). rLMSCs-up grafts transplantation substantially reduced corneal opacity (**B**) and neovascularization (**C**) scores and, at the same time, promoted earlier corneal epithelization (**D**) in the rabbit model of total LSCD compared to the control group ($n = 10$; *$P < 0.05$, ***$P < 0.0002$, ****$P < 0.0001$).

Investigative Ophthalmology & Visual Science

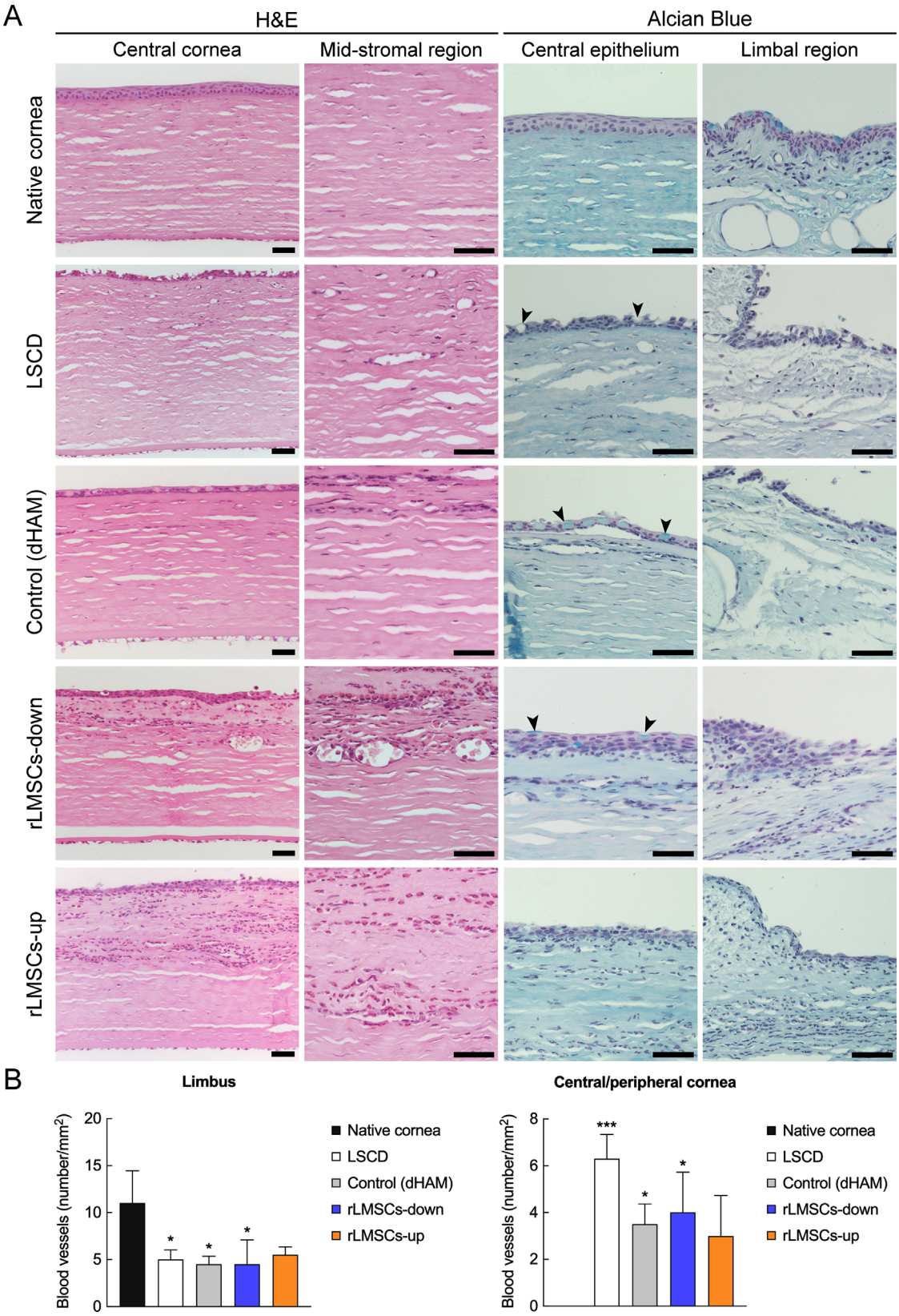

Figure 8. The rLMSCs-up transplantation promotes epithelization in a cornea-like manner. (**A**) Representative H&E and Alcian Blue staining images in 90 days after surgery. Conjunctiva expansion (goblet cells indicated with arrowheads) was observed in the control and rLMSCs-down grafts groups (similar to LSCD) in 90 days after surgery while cornea-like epithelium was found in the rLMSCs-up grafts group. (**B**) Grafts transplantation was followed by the decrease in the number of blood vessels per mm^2 across limbal region and by neovascularization of corneal stroma in the control, rLMSCs-down, and rLMSCs-up grafts groups compared to native cornea. At the same time, there were no statistically significant differences between rLMSCs-up grafts group and native cornea which could be related to the chosen sample size ($n = 3$; $^{*}P < 0.05$, $^{***}P < 0.0002$). Scale bars: 50 µm.

Investigative Ophthalmology & Visual Science

that both rLMSCs and hLMSCs expressed epithelial and mesenchymal markers at P6 in vitro. Especially, CK3/12 and vimentin filaments were found in cultured cells simultaneously. Mesenchymal stem cells of different origins are known to be able to express both epithelial and mesenchymal markers cultured under certain conditions and to be induced to differentiate into epithelial way.[39–41] For instance, Ma et al. successfully used bone marrow-derived mesenchymal stem cells to restore chemically damaged rat corneas.[42] Thus, the co-expression of epithelial and mesenchymal markers in both cultures of rLMSCs and hLMSCs is consistent with the understanding that mesenchymal stem cells could be induced to differentiate into epithelial way and indicates their potential for corneal epithelial reconstruction.

Cell surface markers' expression was similar to other mesenchymal stem cells derived from different tissues in both cultures of rLMSCs and hLMSCs and is consistent with the observations of other authors.[43–46] However, CD146 was not expressed in comparison to the previously reported data, which could be due to the differences among subpopulations of oral mucosa cells.[43]

Karyotypes of both cultures of rLMSCs and hLMSCs were found to be normal. Importantly, no CSCAs as well as the negligible number of NSCAs were observed in the population of hLMSCs compared to rLMSCs which had three times more percentage of NSCAs. Most probably, the low number of abnormalities in hLMSCs karyotype depends on the fact that human cells have more stable genome in comparison to other animal cells. At the same time, it is known that genomes possess plasticity and NSCAs could promote adaptation and survival of cultured cells.[47]

Corneal restoration success after surgery depends on scaffold properties and stem cells used. Here, we demonstrated that rLMSCs seeded onto dHAM promoted corneal epithelial reconstruction in the rabbit model of total LSCD. Particularly, rLMSCs-up grafts transplantation significantly reduced corneal neovascularization and improved corneal clarity. Similar results were reported earlier by other authors.[12,13,16] It should be highlighted that the rLMSCs-up grafts transplantation not only restored corneal integrity but also resulted in the re-epithelization in a cornea-like manner. On the other hand, rLMSCs-down grafts transplantation had similar results to the control group and did not promote any significant changes in corneal clarity and neovascularization. We hypothesize that it could be associated with the blood-mediated inflammation and cell death in the case of rLMSCs were directly contacting damaged eye tissues without being protected with a scaffold.[48,49] Noteworthy, specific infiltration with eosinophils was observed across corneal stroma in all three groups. It was shown recently that 12/15-lipoxygenase-expressing eosinophils are crucial for corneal re-epithelization and could contribute to the corneal wound healing process through the local producing of pro-resolving mediators.[50]

Nevertheless, this study has some limitations. First, we highlighted the importance of chromosomal stability confirmation, however, further investigations, such as tumorigenicity assay, need to be secured to sufficiently demonstrate the inability of cells to oncogenic transformation. Second, the epithelial differentiation of LMSCs was not shown in vitro. Therefore, our conclusions are based on the epithelial markers' expression and histological analysis of rabbit eyes after grafts transplantation. Finally, dHAM was used as the scaffold to transfer rLMSCs on the rabbit corneas. Scaffold properties is known to be crucial for tissue regeneration, especially in terms of corneal transparency. The dHAM is known to decrease corneal transparency via promoting LSCs and keratocytes myofibroblasts transformation.[3] Therefore, alternative scaffolds are expected to be used to achieve more prominent results.

Overall, our findings demonstrate that LMSCs possess high proliferation and differentiation potential as well as maintain chromosomal stability during culturing. The rLMSCs transplantation in the rabbit model of LSCD resulted in the restoration of corneal integrity and structure, indicating the potential of LMSCs for the treatment of corneal diseases and requiring further research.

Acknowledgments

The present work was performed using equipment of the shared research facility "Vertebrate cell culture collection" supported by the Ministry of Science and Higher Education of the Russian Federation (Agreement no. 075-15-2021-683).

Supported by the Ministry of Science and Higher Education Russian Federation Agreement No. 075-15-2020-773.

Disclosure: **K.E. Zhurenkov**, None; **E.I. Alexander-Sinkler**, None; **I.O. Gavrilyik**, None; **N.M. Yartseva**, None; **S.A. Aleksandrova**, None; **T.V. Mashel**, None; **J.I. Khorolskaya**, None; **M.I. Blinova**, None; **A.N. Kulikov**, None; **S.V. Churashov**, None; **V.F. Chernysh**, None; **N.A. Mikhailova**, None

References

1. Maurice DM. The structure and transparency of the cornea. *J Physiol*. 1957;136(2):263–286.
2. Dua HS, Faraj LA, Said DG, Gray T, Lowe J. Human Corneal Anatomy Redefined. *Ophthalmology*. 2013;120(9):1778–1785.
3. Gouveia RM, Lepert G, Gupta S, Mohan RR, Paterson C, Connon CJ. Assessment of corneal substrate biomechanics and its effect on epithelial stem cell maintenance and differentiation. *Nat Commun*. 2019;10(1):1496.
4. Vattulainen M, Ilmarinen T, Koivusalo L, Viiri K, Hongisto H, Skottman H. Modulation of Wnt/BMP pathways during corneal differentiation of hPSC maintains ABCG2-positive LSC population that demonstrates increased regenerative potential. *Stem Cell Res Ther*. 2019;10(1):236.
5. Dua HS, Saini JS, Azuara-Blanco A, Gupta P. Limbal stem cell deficiency: concept, aetiology, clinical presentation, diagnosis and management. *Indian J Ophthalmol*. 2000;48(2):83–92.
6. Haagdorens M, Van Acker SI, Van Gerwen V, et al. Limbal Stem Cell Deficiency: Current Treatment Options and Emerging Therapies. *Stem Cells Int*. 2016;2016:1–22.
7. Feng Y, Borrelli M, Reichl S, Schrader S, Geerling G. Review of Alternative Carrier Materials for Ocular Surface Reconstruction. *Curr Eye Res*. 2014;39(6):541–552.
8. Forni MF, Loureiro RR, Cristovam PC, Bonatti JA, Sogayar MC, Gomes JÁP. Comparison Between Different Biomaterial Scaffolds for Limbal-Derived Stem Cells Growth and Enrichment. *Curr Eye Res*. 2013;38(1):27–34.
9. He H, Yiu SC. Stem cell-based therapy for treating limbal stem cells deficiency: A review of different strategies. *Saudi J Ophthalmol*. 2014;28(3):188–194.
10. Fernandez-Buenaga R, Aiello F, Zaher SS, Grixti A, Ahmad S. Twenty years of limbal epithelial therapy: an update on managing limbal stem cell deficiency. *BMJ Open Ophthalmol*. 2018;3(1):e000164.
11. Ballen PH. Mucous Membrane Grafts in Chemical (Lye) Burns*. *Am J Ophthalmol*. 1963;55(2):302–312.

12. Nakamura T, Endo KI, Cooper LJ, et al. The Successful Culture and Autologous Transplantation of Rabbit Oral Mucosal Epithelial Cells on Amniotic Membrane. *Investig Opthalmology Vis Sci*. 2003;44(1):106.
13. Nakamura T, Takeda K, Inatomi T, Sotozono C, Kinoshita S. Long-term results of autologous cultivated oral mucosal epithelial transplantation in the scar phase of severe ocular surface disorders. *Br J Ophthalmol*. 2011;95(7):942–946.
14. Nakamura T, Yokoo S, Bentley AJ, et al. Development of functional human oral mucosal epithelial stem/progenitor cell sheets using a feeder-free and serum-free culture system for ocular surface reconstruction. *Sci Rep*. 2016;6(1):37173.
15. Utheim TP. Concise Review: Transplantation of Cultured Oral Mucosal Epithelial Cells for Treating Limbal Stem Cell Deficiency-Current Status and Future Perspectives: Oral Mucosal Epithelial Cells for Treating Limbal Stem Cell Deficiency. *Stem Cells*. 2015;33(6):1685–1695.
16. Paaske Utheim T, Aass Utheim Ø, Khan QES, Sehic A. Culture of Oral Mucosal Epithelial Cells for the Purpose of Treating Limbal Stem Cell Deficiency. *J Funct Biomater*. 2016;7(1):5.
17. Nanci A, TenCate AR. *Ten Cate's Oral Histology: Development, Structure, and Function*. 9th edition. New York, NY: Elsevier; 2018.
18. Krylova TA, Kol'tsova AM, Zenin VV, Musorina AS, Iakovleva TK, Polianskaia GG. [Comparative characteristics of new mesenchymal stem cell lines derived from human embryonic stem cells, bone marrow and foreskin]. *Tsitologiia*. 2012;54(1):5–16.
19. Franken NAP, Rodermond HM, Stap J, Haveman J, van Bree C. Clonogenic assay of cells in vitro. *Nat Protoc*. 2006;1(5):2315–2319.
20. MacLeod RAF, Drexler HG. Cytogenetic Analysis of Cell Lines. In: *Basic Cell Culture Protocols*. Vol. 290. New York, NY: Humana Press; 2004:051–070.
21. Özkinay C, Mitelman F. A simple trypsin-Giemsa technique producing simultaneous G- and C-banding in human chromosomes. *Hereditas*. 2009;90(1):1–4.
22. Standard karyotype of the laboratory rabbit, Oryctolagus cuniculus. *Cytogenet Genome Res*. 1981;31(4):240–248.
23. International Standing Committee on Human Cytogenetic Nomenclature, Shaffer LG, Slovak ML, Campbell LJ, eds. *ISCN 2009: An International System for Human Cytogenetic Nomenclature (2009)*. Unionville, CT: Karger; 2009.
24. Aleksandrova O, Gavrilyik I, Mashel T, et al. The preparation of the amniotic membrane as a scaffold cell cultures for the bioengineered corneal structures (in Russian). *Saratov J Med Sci Res*. 2019;15(2):409–413.
25. Dubovikov A, Gavrilyik I, Kulikov A, et al. Method of immobilization of native amniotic membrane for transportation, preservation and its application as a carrier of cultured cells. Available at: https://patents.google.com/patent/RU2646162C1/en. Published online February 21, 2019.
26. Voino-Yasenetsky V. *The proliferation and variability of the eye tissues in diseases and injuries (in Russian)*. Moscow, Russia: Vysshaya Shkola; 1979.
27. Inatomi T, Nakamura T, Koizumi N, Sotozono C, Yokoi N, Kinoshita S. Midterm Results on Ocular Surface Reconstruction Using Cultivated Autologous Oral Mucosal Epithelial Transplantation. *Am J Ophthalmol*. 2006;141(2):267–275.e1.
28. Sukhinin M. V. Morphological characterization of the anterior corneal epithelium and the vascular bed of the conjunctiva of the eye in normal conditions and with the mechanically damaged perilimbal zone (in Russian). MD thesis. S. M. Kirov Military Medical Academy; 2011, https://www.dissercat.com/content/morfologicheskaya-kharakteristika-perednego-epiteliya-rogovitsy-i-sosudistogo-rusla-konyunkt.
29. Schwab KE, Gargett CE. Co-expression of two perivascular cell markers isolates mesenchymal stem-like cells from human endometrium. *Hum Reprod*. 2007;22(11):2903–2911.
30. Aravena C, Bozkurt K, Chuephanich P, Supiyaphun C, Yu F, Deng SX. Classification of Limbal Stem Cell Deficiency Using Clinical and Confocal Grading. *Cornea*. 2019;38(1):1–7.
31. Kolli S, Ahmad S, Mudhar HS, Meeny A, Lako M, Figueiredo FC. Successful Application of Ex Vivo Expanded Human Autologous Oral Mucosal Epithelium for the Treatment of Total Bilateral Limbal Stem Cell Deficiency: OME Transplantation in Patients with Bilateral LSCD. *Stem Cells*. 2014;32(8):2135–2146.
32. Polianskaia GG. [The problem of genomic instability of cultivated human stem cells]. *Tsitologiia*. 2014;56(10):697–707.
33. Scheers I, Lombard C, Paganelli M, et al. Human Umbilical Cord Matrix Stem Cells Maintain Multilineage Differentiation Abilities and Do Not Transform during Long-Term Culture. Lionetti V, ed. *PLoS One*. 2013;8(8):e71374.
34. Campisi J. Replicative Senescence: An Old Lives' Tale? *Cell*. 1996;84(4):497–500.
35. Schlötzer-Schrehardt U, Kruse FE. Identification and characterization of limbal stem cells. *Exp Eye Res*. 2005;81(3):247–264.
36. Guo Z, Zhang W, Jia Y, Liu Q, Li Z, Lin J. An Insight into the Difficulties in the Discovery of Specific Biomarkers of Limbal Stem Cells. *Int J Mol Sci*. 2018;19(7):1982.
37. Priya CG, Arpitha P, Vaishali S, et al. Adult human buccal epithelial stem cells: identification, ex-vivo expansion, and transplantation for corneal surface reconstruction. *Eye*. 2011;25(12):1641–1649.
38. Ashery-Padan R, Marquardt T, Zhou X, Gruss P. Pax6 activity in the lens primordium is required for lens formation and for correct placement of a single retina in the eye. *Genes Dev*. 2000;14(21):2701–2711.
39. Xie HT, Chen SY, Li GG, Tseng SCG. Isolation and Expansion of Human Limbal Stromal Niche Cells. *Investig Opthalmol Vis Sci*. 2012;53(1):279.
40. Li GG, Zhu YT, Xie HT, Chen SY, Tseng SCG. Mesenchymal Stem Cells Derived from Human Limbal Niche Cells. *Investig Opthalmol Vis Sci*. 2012;53(9):5686.
41. Khorolskaya JI, Perepletchikova DA, Kachkin DV, et al. Derivation and Characterization of EGFP-Labeled Rabbit Limbal Mesenchymal Stem Cells and Their Potential for Research in Regenerative Ophthalmology. *Biomedicines*. 2021;9(9):1134.
42. Ma Y, Xu Y, Xiao Z, et al. Reconstruction of Chemically Burned Rat Corneal Surface by Bone Marrow–Derived Human Mesenchymal Stem Cells. *Stem Cells*. 2006;24(2):315–321.
43. Higa K, Satake Y, Shimazaki J. The characterization of human oral mucosal fibroblasts and their use as feeder cells in cultivated epithelial sheets. *Future Sci OA*. 2017;3(4):FSO243.
44. Dominici M, Le Blanc K, Mueller I, et al. Minimal criteria for defining multipotent mesenchymal stromal cells. The International Society for Cellular Therapy position statement. *Cytotherapy*. 2006;8(4):315–317.
45. Lee TC, Lee TH, Huang YH, et al. Comparison of Surface Markers between Human and Rabbit Mesenchymal Stem Cells. Zhou F, ed. *PLoS One*. 2014;9(11):e111390.
46. Battula VL, Treml S, Bareiss PM, et al. Isolation of functionally distinct mesenchymal stem cell subsets using antibodies against CD56, CD271, and mesenchymal stem cell antigen-1. *Haematologica*. 2009;94(2):173–184.

Investigative Ophthalmology & Visual Science

47. Heng HHQ, Regan SM, Liu G, Ye CJ. Why it is crucial to analyze non clonal chromosome aberrations or NCCAs? *Mol Cytogenet*. 2016;9(1):15, s13039-016-0223-2.
48. Calonge M, Pérez I, Galindo S, et al. A proof-of-concept clinical trial using mesenchymal stem cells for the treatment of corneal epithelial stem cell deficiency. *Transl Res*. 2019;206:18–40.
49. Cinat D, Coppes RP, Barazzuol L. DNA Damage-Induced Inflammatory Microenvironment and Adult Stem Cell Response. *Front Cell Dev Biol*. 2021;9:729136.
50. Ogawa M, Ishihara T, Isobe Y, et al. Eosinophils promote corneal wound healing via the 12/15-lipoxygenase pathway. *FASEB J*. 2020;34(9):12492–12501.

Investigative Ophthalmology & Visual Science